

An Efficient and Reusable Multifunctional Composite Magnetic Nanocatalyst for Knoevenagel Condensation

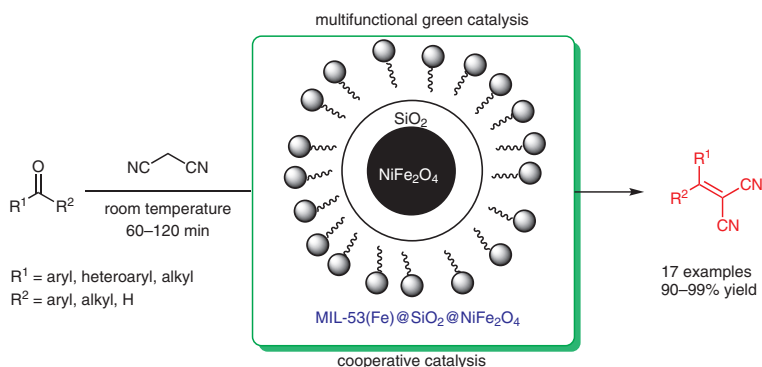
Nan Yao

Jin Tan

Yang Liu

Yu Lin Hu* 

College of Materials and Chemical Engineering, Key Laboratory of Inorganic Nonmetallic Crystalline and Energy Conversion Materials, China Three Gorges University, Yichang 443002, P. R. of China
 huyulin@ctgu.edu.cn
 huyulin1982@163.com



Received: 25.11.2018

Accepted after revision: 21.12.2018

Published online: 06.03.2019

DOI: 10.1055/s-0037-1612076; Art ID: st-2018-k0766-l

Abstract A range of multifunctional magnetic metal–organic framework nanomaterials consisting of various mass ratios of the metal–organic framework MIL-53(Fe) and magnetic $\text{SiO}_2@NiFe_2O_4$ nanoparticles were designed, prepared, characterized, and evaluated as heterogeneous catalysts for the Knoevenagel condensation. The as-fabricated nanomaterials, especially the nanocatalyst $MIL-53(Fe)@SiO_2@NiFe_2O_4(1.0)$, showed good catalytic performance in the Knoevenagel condensation at room temperature as a result of synergistic interaction between the Lewis acid iron sites of MIL-53(Fe) and the active sites of the magnetic $\text{SiO}_2@NiFe_2O_4$ nanoparticles. In addition, the heterogeneous catalyst was readily recovered and a recycling test showed that it could be reused for five times without significant loss of its catalytic activity, making it economical and environmentally friendly.

Key words metal-organic frameworks, magnetic nanocatalyst, Knoevenagel condensation, cooperative catalysis, heterogeneous catalysis, iron catalysis

Knoevenagel condensation is one of the most important and challenging C–C bond-forming reactions, as the α,β -unsaturated products have extensive applications in the production of fine chemicals and intermediates.^{1,2} Knoevenagel condensations are normally catalyzed by base catalysts in liquid-phase systems under homogeneous conditions.^{1,3} Unfortunately, the separation and handling of waste materials generated under these conditions creates undesirable economic and environmental problems. Consequently, there is an urgent need to develop new and efficient heterogeneous catalytic systems to perform these transformations. In this regard, a number of representative heterogeneous catalysts have been developed for the Knoevenagel condensation, including phosphotungstic acid immobilized on mesoporous graphitic carbon nitride ($g-C_3N_4$),⁴ Ni/SiO_2 ,⁵ $g-C_3N_4$,⁶ aziridine-functionalized multiwalled carbon nanotubes,⁷ triethylenetetramine-functionalized polyacryloni-

trile fiber,⁸ rhodium–platinum nanoparticles supported on thiocarbamide-functionalized graphene oxide,⁹ a core–shell silica-layered double hydroxide,¹⁰ ionic liquids,^{11–13} and others.^{14–18} Most of these catalysts are efficient but, nevertheless, suffer from various limitations, such as a relative lack of availability or environmental contamination. Therefore, the development of more-sustainable and more-efficient catalysts for the Knoevenagel condensation continues to be a challenging goal.

Metal–organic frameworks (MOFs), as a class of fascinating functional materials, have attracted considerable attention due to their intriguing structural diversity, versatile physical and chemical properties, and potential extensive applications in the fields of catalysis and chemical transformation.^{19–21} Although some MOFs exhibit good catalytic activities for the Knoevenagel condensation,^{22–25} most have drawbacks in terms of costly separation and a lack of recyclability. Consequently, there is a considerable demand for the development of MOF-based heterogeneous catalysts that are more environmentally benign and more efficient.

In recent years, magnetic nanoparticles have attracted broad attention owing to their unique high surface area, ordered pore arrangement, and superparamagnetic properties.^{26,27} An inherent advantage of magnetic nanoparticles is the ease with which they can be recovered and separated for subsequent reuse in chemical transformations, simply by using an external magnet and decantation. Furthermore, it has been found that the stability, dispersibility, and catalytic properties of MOFs can be enhanced by imparting magnetic properties to the framework.^{28,29} Therefore, MOF catalysts containing magnetic nanoparticles might exhibit an outstanding catalytic performance as a result the combination of the advantageous properties of the two materials.

On the basis of the aforementioned considerations, we report on the use of a combination of nickel ferrite ($NiFe_2O_4$) magnetic nanoparticles with an MIL-53(Fe) MOF

to form a new multifunctional magnetic MOF catalysts. Magnetic nanomaterials MIL-53(Fe)@SiO₂@NiFe₂O₄ containing various quantities of MIL-53(Fe) encapsulated on the surface of SiO₂@NiFe₂O₄ were examined as efficient and environmentally friendly catalysts for Knoevenagel condensations under mild conditions. The recyclability and reusability of the nanocatalysts were also examined.

The as-synthesized nanomaterials were characterized by means of FTIR, XRD, SEM, UV/vis, N₂ physisorption, and XPS analyses. FTIR spectra of the nanomaterials are shown in Figure S1 of the Supplementary Information (SI). The characteristic peaks at about 1631 and 762 cm⁻¹ were attributed to the C=C and C-H stretching vibrations of the benzene ring of MIL-53(Fe), whereas those at about 1542 and 1397 cm⁻¹ were attributed to O-C-O stretching vibrations of the carboxyl groups of MIL-53(Fe).^{29–33} The characteristic bands at about 3446 and 952 cm⁻¹ were ascribed to the stretching vibration of OH and Si-OH, respectively, whereas the band at about 1085 cm⁻¹ was ascribed to the stretching vibration of Si-O-Si.^{30,31} The peak at 596 cm⁻¹ is related to typical stretching vibrational modes of Fe-O.^{34,35} The results for the characteristic vibrational peaks of the as-synthesized products therefore confirmed the successful formation of the magnetic nanomaterials.

Figure S2 in the SI shows the XRD patterns of the prepared nanomaterials. The diffraction peaks observed at 9.4, 12.9, and 17.8° belonged to typical patterns of crystalline MIL-53(Fe).^{36,37} The six typical diffraction peaks of nanomaterials were observed at 2θ = 30.4, 35.2, 42.7, 53.8, 57.4, and 52.3°; these can be assigned, respectively, to the (220), (311), (400), (422), (511), and (440) reflections of magnetic NiFe₂O₄ nanoparticles [JCPDS No. 10-0325].^{34,35} These results indicated the presence of a highly ordered mesoporous structure, and confirmed that the magnetic nanomaterials had been successfully formed. The characteristic peaks of NiFe₂O₄ were retained after encapsulation with MIL-53(Fe), indicating that the crystal structure of NiFe₂O₄ was maintained and intact during the synthesis process.

Scanning electron microscopy (SEM) images of the as-synthesized nanomaterials are shown in Figure S3 of the SI. Micrograph (d) shows the presence of well-ordered arrays of SiO₂@NiFe₂O₄ nanoparticles, typical of the morphology of magnetic particles.^{34,35} It could be clearly observed that the morphologies of the magnetic MIL-53(Fe) nanomaterials consisted of agglomerations of small spheres of uniform nanometer-sized particles.

Figure S4 of the SI shows the diffuse reflectance UV-vis spectra of the prepared nanomaterials. The broad distinct absorption peak at 210–230 nm was attributed to the characteristic absorption properties of SiO₂@NiFe₂O₄.^{30,34,35} No other typical absorption peaks were found on the patterns of the nanomaterials MIL-53(Fe)@SiO₂@NiFe₂O₄, indicating the absence of extra-crystal framework and a highly uniform distribution of species in these mesoporous frameworks.

N₂ adsorption-desorption measurements are a powerful tool for the characterization of nanomaterials. Figure S5 of the SI shows the isotherms and pore-size distribution of the prepared nanomaterial MIL-53(Fe)@SiO₂@NiFe₂O₄(1.0). It is clear that MIL-53(Fe)@SiO₂@NiFe₂O₄(1.0) has a BET surface area of 102.86 m²·g⁻¹ and a total pore volume of 0.5329 cm³·g⁻¹. The pore-size distribution confirms that well defined pores with a pore-size distribution of 2.12 nm are present in this nanomaterial. These results show that this nanomaterial exhibits a Type I isotherm, characteristic of highly ordered mesoporous materials.^{28,29}

To obtain additional information about the elemental composition and the chemical nature of the active species in the nanocatalyst MIL-53(Fe)@SiO₂@NiFe₂O₄(1.0), we performed XPS studies. As shown in Figure S6 of the SI, the nanocatalyst consisted of C, O, Si, Fe and Ni, and the peaks corresponding to C1s, O1s, Si2p, Fe2p, and Ni2p appeared at 284.6, 531.1, 102.6, 711.6, and 856.5 eV, respectively.^{27,30,31} The XPS results provided further confirmation of the structure of the nanocatalyst MIL-53(Fe)@SiO₂@NiFe₂O₄(1.0), and were consistent with the XRD and FTIR analyses.

To examine the catalytic activity of the nanomaterials MIL-53(Fe)@SiO₂@NiFe₂O₄, we chose the Knoevenagel condensation of benzaldehyde with malononitrile as a model reaction. Initially, we examined the catalytic activities of MIL-53(Fe)@SiO₂@NiFe₂O₄ nanocatalysts with various mass ratios of MIL-53(Fe) and SiO₂@NiFe₂O₄: MIL-53(Fe)@SiO₂@NiFe₂O₄(0.5), MIL-53(Fe)@SiO₂@NiFe₂O₄(1.0), and MIL-53(Fe)@SiO₂@NiFe₂O₄(1.5) (Table 1, entries 1–3). Among these nanocatalysts, MIL-53(Fe)@SiO₂@NiFe₂O₄(1.0) was the most effective catalyst, affording a conversion of >99% and a product yield of 98% (Table 1, entry 2). These results indicated that the heterogeneous nanocatalyst MIL-53(Fe)@SiO₂@NiFe₂O₄(1.0) has excellent catalytic activity for the condensation. This catalyst has sufficiently active sites for the reaction, probably as a result of synergy between the active sites of MIL-53(Fe) and those of the magnetic SiO₂@NiFe₂O₄ particles. The amount of catalyst also influenced the outcome of the condensation reaction. On increasing the amount of nanocatalyst to 0.1 g, an increase in the conversion and the product yield were observed (Table 1, entries 2 and 6–8), whereas a further increase to 0.15 g did not significantly improve the conversion and yield (Table 1, entry 9). It is a promising result that MIL-53(Fe)@SiO₂@NiFe₂O₄(1.0) exhibited a high catalytic activity at a low catalyst loading 0.1 g in the catalytic reaction. For comparison, the condensation was also performed by using SiO₂@NiFe₂O₄ alone or bulk MIL-53(Fe) as the catalyst (Table 1, entries 4 and 5, respectively). When SiO₂@NiFe₂O₄ was used alone, only 80% product yield and 82% conversion were obtained (Table 1, entry 4), whereas the use of bulk MIL-53(Fe) as the catalyst afforded a much more lower product yield (72%) and conversion (74%) (Table 1, entry 5). Therefore, MIL-53(Fe)@SiO₂@NiFe₂O₄(1.0) is a suitable nanocatalyst for the condensation.

Table 1 Catalyst Screening for the Knoevenagel Condensation of Benzaldehyde and Malononitrile^a

Entry	Catalyst	Amount (g)	Time (min)	Conversion ^b (%)	Yield ^c (%)
1	MIL-53(Fe)@SiO ₂ @NiFe ₂ O ₄ (0.5)	0.10	60	91	89
2	MIL-53(Fe)@SiO ₂ @NiFe ₂ O ₄ (1.0)	0.10	60	>99	98
3	MIL-53(Fe)@SiO ₂ @NiFe ₂ O ₄ (1.5)	0.10	60	>99	99
4	SiO ₂ @NiFe ₂ O ₄	0.10	120	82	80
5	MIL-53(Fe)	0.10	120	74	72
6	–	–	240	–	–
7	MIL-53(Fe)@SiO ₂ @NiFe ₂ O ₄ (1.0)	0.05	90	82	81
8	MIL-53(Fe)@SiO ₂ @NiFe ₂ O ₄ (1.0)	0.08	60	94	93
9	MIL-53(Fe)@SiO ₂ @NiFe ₂ O ₄ (1.0)	0.15	60	>99	98

^a Reaction conditions: PhCHO (5 mmol), malononitrile (5 mmol), EtOH (15 mL), catalyst, r.t.

^b Determined by HPLC analysis of the crude reaction mixture.

^c Isolated yield.

The stability and reusability of a heterogeneous catalyst are important factors in terms of its practical applications. The thermal stability of nanocatalyst MIL-53(Fe)@SiO₂@NiFe₂O₄(1.0) was examined by thermogravimetry (SI; Figure S7). The small weight loss below 100 °C was the result of desorption of water adsorbed on the surface of the sample. The marked mass loss of about 12% between 200 and 500 °C was attributed to breakdown of organic moieties. These results showed that the nanocatalyst is thermally stable below about 200 °C, which is beneficial in terms of its reusability. The magnetization curve of the nanocatalyst MIL-53(Fe)@SiO₂@NiFe₂O₄(1.0), shown in Figure S8 of the SI, confirmed that the material has typical superparamagnetic properties with a saturation magnetization of 24.3 emu·g⁻¹, which is sufficient to permit magnetic separation of the solid nanocatalyst.

Next, we examined the recyclability of the nanocatalyst MIL-53(Fe)@SiO₂@NiFe₂O₄(1.0) in the Knoevenagel condensation of benzaldehyde and malononitrile under the optimized catalytic reaction conditions (SI; Figure S9). The catalyst was easily separated by using an external magnet with simple decantation and, when washed several times with EtOH, could be reused directly for successive experimental runs. We found that the recycled catalyst could be reused in five reaction cycles with negligible loss of its catalytic activity, thereby confirming the excellent catalytic activity, stability, and reusability of this nanocatalyst. SEM of the reused MIL-53(Fe)@SiO₂@NiFe₂O₄(1.0) after five runs indicated that the morphology and highly ordered nanostructure of the catalyst were maintained during the course of the condensation (SI; Figure S3e). XRD spectra of the reused catalyst after five runs were similar to those of the fresh catalysts, indicating that no obvious change in the crystal structure of the catalyst occurred during the condensation (SI; Figure S10).

To confirm the efficiency and capabilities of our MIL-53(Fe)@SiO₂@NiFe₂O₄(1.0) catalyst, we compared its catalytic activity in the heterogeneous condensation of benzaldehyde and malononitrile with that of other reported heterogeneous catalysts (SI; Table S1). Our catalytic system showed promising features in terms of its high activity and efficiency, producing high to excellent yields under mild reaction conditions. These results therefore confirm that MIL-53(Fe)@SiO₂@NiFe₂O₄(1.0) is a practical and suitable magnetic MOF nanocatalyst for the Knoevenagel condensation.

Encouraged by the above results, we evaluated the catalytic activities of MIL-53(Fe)@SiO₂@NiFe₂O₄(1.0) for the heterogeneous condensations of various aldehydes and ketones with malononitrile under the optimized conditions, and the results are listed in Table S2 of the SI. Various aryl aldehydes and ketones were smoothly converted into the desired products in high to excellent yields within short reaction times (60–120 min).³⁸ To our delight, both electron-deficient and electron-rich aryl aldehydes delivered the corresponding products in an isolated yield of 93–99% (SI; Table S2, entries 1–10). Even aryl aldehydes bearing strongly electron-withdrawing nitro or carboxy groups reacted readily and efficiently to afford the desired products in excellent yields (SI; Table S2, entries 6 and 7). Note that the reaction rates of ketones were slower than those of aldehydes and that longer reaction times were needed to obtain good to excellent yields (SI; Table S2, entries 11–17). It is also interesting to note that the reaction of malononitrile with hexane-2,5-dione (SI; Table S2, entries 14 and 15) gave the dicondensation product 2,5-dimethylhexa-1,5-diene-1,1,6,6-tetracarbonitrile exclusively, whereas pentane-2,4-dione gave the monocondensation product (1-methyl-3-oxobutylidene)malononitrile (Table S2, entry 16). These results confirm the high efficiency and versatility of our designed nanocatalyst in all cases.

In conclusion, a range of multifunctional magnetic MOF nanomaterials with various mass ratios of MIL-53(Fe) to magnetic $\text{SiO}_2@NiFe_2O_4$ nanoparticles were synthesized, characterized, and used as novel heterogeneous catalysts for the Knoevenagel condensation. The presence of synergistic effects between the Lewis acid iron sites of MIL-53(Fe) and the basic sites of magnetic $\text{SiO}_2@NiFe_2O_4$ nanoparticles in the nanomaterials makes them suitable as active catalysts for the condensation. Our studies showed that the multifunctional cooperative nanocatalyst MIL-53(Fe) $@SiO_2@NiFe_2O_4(1.0)$ has a higher activity than other catalysts in this reaction. The present method provides an operationally simple, highly efficient, and environmentally benign alternative for the Knoevenagel condensation. Furthermore, our heterogeneous catalyst shows excellent reusability and can be reused for five runs with negligible loss of its activity. The advantages of the present method are the high catalytic activity, easy workup, excellent reusability, and green and environmentally benign nature.

Funding Information

This work was supported by the National Natural Science Foundation of China (21506115) and Excellent Dissertation of China Three Gorges University (2018SSPY055).

Supporting Information

Supporting information for this article is available online at <https://doi.org/10.1055/s-0037-1612076>.

References and Notes

- Vekariya, R. H.; Patel, H. D. *Synth. Commun.* **2014**, *44*, 2756.
- Krawczyk, H.; Albrecht, L. *Synthesis* **2005**, 2887.
- Raychev, P. D.; Roussi, L.; Dutasta, J. P.; Martinez, A.; Dufaud, V. *Catal. Commun.* **2012**, *28*, 1.
- Wang, H.; Wang, C.; Yang, Y.; Zhao, M.; Wang, Y. *Catal. Sci. Technol.* **2017**, *7*, 405.
- Pullabhotla, V. S. R. R.; Rahman, A.; Jonnalagadda, S. B. *Catal. Commun.* **2009**, *10*, 365.
- Sharma, P.; Sasson, Y. *RSC Adv.* **2017**, *7*, 25589.
- Tuci, G.; Luconi, L.; Rossin, A.; Berretti, E.; Ba, H.; Innocenti, M.; Yakhvarov, D.; Caporali, S.; Pham-Huu, C.; Giambastiani, G. *ACS Appl. Mater. Interfaces* **2016**, *8*, 30099.
- Li, G.; Xiao, J.; Zhang, W. *Green Chem.* **2012**, *14*, 2234.
- Şen, B.; Akdere, E.-H.; Şavk, A.; Gültekin, E.; Paralı, Ö.; Göksu, H.; Şen, F. *Appl. Catal., B* **2018**, *225*, 148.
- Shirotori, M.; Nishimura, S.; Ebitani, K. *J. Mater. Chem. A* **2017**, *5*, 6947.
- del Hierro, I.; Pérez, Y.; Fajardo, M. *Mol. Catal.* **2018**, *450*, 112.
- Boroujeni, K. P.; Jafarinasab, M. *Chin. Chem. Lett.* **2012**, *23*, 1067.
- Elhamifar, D.; Kazemipoor, S. J. *Mol. Catal. A: Chem.* **2016**, *415*, 74.
- Xu, G.; Wang, L.; Li, M.; Tao, M.; Zhang, W. *Green Chem.* **2017**, *19*, 5818.
- Calvino-Casilda, V.; Olejniczak, M.; Martín-Aranda, R. M.; Ziolk, M. *Microporous Mesoporous Mater.* **2016**, *224*, 201.
- Varadwaj, G. B. B.; Rana, S.; Parida, K. M. *Dalton Trans.* **2013**, *42*, 5122.
- Franconetti, A.; Domínguez-Rodríguez, P.; Lara-García, D.; Prado-Gotor, R.; Cabrera-Escribano, F. *Appl. Catal., A* **2016**, *517*, 176.
- Li, Q.; Wang, X.; Yu, Y.; Chen, Y.; Dai, L. *Tetrahedron* **2016**, *72*, 8358.
- Xu, W.; Thapa, K. B.; Ju, Q.; Fang, Z.; Huang, W. *Coord. Chem. Rev.* **2018**, *373*, 199.
- Schneemann, A.; Bon, V.; Schwedler, I.; Senkovska, I.; Kaskel, S.; Fischer, R. A. *Chem. Soc. Rev.* **2014**, *43*, 6062.
- Zhou, W.; Wu, Y.-P.; Wang, X.; Tian, J.-W.; Huang, D.-D.; Zhao, J.; Lan, Y.-Q.; Li, D.-S. *CrystEngComm* **2018**, *20*, 4804.
- Zhang, Y.; Wang, Y.; Liu, L.; Wei, N.; Gao, M.-L.; Zhao, D.; Han, Z.-B. *Inorg. Chem.* **2018**, *57*, 2193.
- Ezugwu, C. I.; Mousavi, B.; Asraf, M. A.; Luo, Z.; Verpoort, F. *J. Catal.* **2016**, *344*, 445.
- Rambabu, D.; Ashraf, M.; Pooja, Gupta, A.; Dhir, A. *Tetrahedron Lett.* **2017**, *58*, 4691.
- Opanasenko, M.; Dhakshinamoorthy, A.; Shamzhy, M.; Nachtigall, P.; Horáček, M.; Garcia, H.; Čejka, J. *Catal. Sci. Technol.* **2013**, *3*, 500.
- Zhang, L.; He, Y.; Yang, X.; Yuan, H.; Du, Z.; Wu, Y. *Chem. Eng. J. (Amsterdam, Neth.)* **2015**, *278*, 129.
- Baig, R. B. N.; Nadagouda, M. N.; Varma, R. S. *Coord. Chem. Rev.* **2015**, *287*, 137.
- Babazadeh, M.; Hosseinzadeh-Khanmiri, R.; Abolhasani, J.; Ghorbani-Kalhor, E.; Hassanpour, A. *RSC Adv.* **2015**, *5*, 19884.
- Yang, Q.; Zhu, Y.; Luo, B.; Lan, F.; Wu, Y.; Gu, Z. *Nanoscale* **2017**, *9*, 527.
- Wang, H.; Zhang, W.; Zhang, F.; Cao, Y.; Su, W. *J. Magn. Magn. Mater.* **2008**, *320*, 1916.
- Liu, Y.; Cherkasov, N.; Gao, P.; Fernández, J.; Lees, M. R.; Rebrov, E. V. *J. Catal.* **2017**, *355*, 120.
- Wang, G.-H.; Lei, Y.-Q.; Song, H.-C. *Anal. Methods* **2014**, *6*, 7842.
- Yang, Q.; Wang, J.; Chen, X.; Yang, W.; Pei, H.; Hu, N.; Li, Z.; Suo, Y.; Li, T.; Wang, J. *J. Mater. Chem. A* **2018**, *6*, 2184.
- Parmekar, M. V.; Salker, A. V. *RSC Adv.* **2016**, *6*, 108458.
- Blanco-Gutierrez, V.; Virumbrales, M.; Saez-Puche, R.; Torralvo-Fernandez, M. J. *J. Phys. Chem. C* **2013**, *117*, 20927.
- Shigematsu, A.; Yamada, T.; Kitagawa, H. *J. Am. Chem. Soc.* **2011**, *133*, 2034.
- Dong, W.; Liu, X.; Shi, W.; Huang, Y. *RSC Adv.* **2015**, *5*, 17451.
- 2-Benzylidenemalononitrile; Typical Procedure**
A mixture of PhCHO (5 mmol), malononitrile (5 mmol), EtOH (15 mL), and MIL-53(Fe) $@SiO_2@NiFe_2O_4(1.0)$ (0.1 g) was magnetically stirred at r.t. until the reaction was complete (TLC). The catalyst that precipitated out from the mixture was collected by using an external magnet, washed with EtOH, and reused for consecutive cycles under the same reaction conditions. The product was crystallized from EtOH to give a white solid; yield: 755 mg (98%); mp 83.8–84.1 °C. ¹H NMR (400 MHz, CDCl₃): δ = 7.47–7.64 (m, 3 H, Ar-H), 7.78 (s, 1 H, CH), 7.85–7.94 (m, 2 H, Ar-H). MS: *m/z* [M + H]⁺ calcd for C₁₀H₇N₂: 155.1; found: 155.06; Anal. Calcd for C₁₀H₆N₂: C, 77.87; H, 3.90; N, 18.15. Found: C, 77.91; H, 3.92; N, 18.17.